Astronomy in Focus, XXIXB, Focus Meeting 6
XXIXth IAU General Assembly, August 2015
Piero Benvenuti, ed.

doi:10.1017/S1743921316004543

Cluster Physics & Evolution

Daisuke Nagai[1], Monique Arnaud[2], Sarthak Dasadia[3], Michael McDonald[4], Ikuyuki Mitsuishi[5] and Andrea Morandi[3] (Editor)

[1]Department of Physics, Yale University, New Haven, CT 06520, U.S.A.

[2]Laboratoire AIM, IRFU/Service d'Astrophysique - CEA/DSM - CNRS - Universitê Paris Diderot, Baî. 709, CEA-Saclay, F-91191 Gif-sur- Yvette Cedex, France

[3]Physics Department, University of Alabama in Huntsville, Huntsville, AL 35899, USA

[4]Kavli Institute for Astrophysics and Space Research, Massachusetts Institute of Technology, 77 Massachusetts Avenue, Cambridge, MA 02139, USA

[5]Nagoya University, Furo-cho, Chikusa-ku, Nagoya, Aichi 464-8602, Japan

Abstract. Recent advances in X-ray and microwave observations have provided unprecedented insights into the structure and evolution of the hot X-ray emitting plasma from their cores to the virialization region in outskirts of galaxy clusters. Recent Sunyaev-Zel'dovich (SZ) surveys (ACT, Planck, SPT) have provided new cluster catalogs, significantly expanding coverage of the mass-redshift plane, while *Chandra* and *XMM-Newton* X-ray follow-up programs have improved our understanding of cluster physics and evolution as well as the surveys themselves. However, the current cluster-based cosmological constraints are still limited by uncertainties in cluster astrophysics. In order to exploit the statistical power of the current and upcoming X-ray and microwave cluster surveys, it is critical to improve our understanding of the structure and evolution of the hot X-ray emitting intracluster medium (ICM). In this session, we discussed recent advances in observations and simulations of galaxy clusters, with highlights on (I) the evolution of ICM profiles and scaling relations, (II) physical processes operating in the outskirts of galaxy clusters, and (III) impact of mergers on the ICM structure in groups and clusters.

Keywords. X-rays: galaxies: clusters, galaxies: clusters: general, galaxies: interactions

1. Cluster Physics and Evolution from new X-ray-SZ cluster samples

Monique Arnaud summarized how the recent arrival of large-area SZ galaxy clusters surveys, by ACT (Marriage *et al.* 2011; Hasselfield *et al.* 2013), SPT (Bleem *et al.* 2015) and *Planck* (PC11a; PC13b; PC15), has resulted in a rapid growth in the number of known, massive galaxy clusters at $z > 0.5$ – a regime which was classified as "high redshift" by the galaxy cluster community as recently as a decade ago due to the paucity of known systems at these redshifts. SZ surveys have the advantage over more traditional cluster-detection methods (e.g., X-ray, optical, near-IR) in that they are roughly redshift independent, selecting only on mass. This results in cleanly selected samples spanning a large range in redshift. There is also a strong complementarity in the coverage of the mass-redshift plan between the new SZ surveys and their X-ray counterparts. The spatial resolution of ACT and SPT ($\sim 1'$) allows them to probe the cluster population above a nearly constant mass threshold up to very high redshift, $z \sim 1.5$, but their smaller area limits the number of high mass objects. *Planck*'s lower spatial resolution ($\sim 5'$) is offset by its being the first all-sky blind survey since the *ROSAT* All Sky Survey (RASS). Although less sensitive, it is uniquely suited to finding high mass, high redshift systems. At the time of writing, there are 135/55/25 confirmed *Planck* clusters with measured redshift $z \geqslant 0.5/0.6/0.7$ with a median $M_{500} = 6.4/6.3/6.1 \times 10^{14} M_{\odot}$. Deep *XMM-Newton* serendipitous surveys (e.g., XCS, Mehrtens *et al.* 2012) or pointings

surveys (Clerc *et al.* 2014, also a talk by Nicolas Clerc) suffer from their limited area but complement the SZ surveys by their still higher sensitivity, allowing the detection of very low mass objects up to $z \sim 1$ and beyond.

Multi-wavelength observations are needed to fully exploit the SZ discoveries. The first *Planck* publications made extensive use of *XMM-Newton* archival data in conjunction with an *XMM-Newton* validation program (PC11b, PC11c). A large *XMM-Newton* and *Chandra* effort has swung into action since the release of the first SZ catalogues, both to complement archival data at low z (which are biased towards known X–ray clusters) and to study evolution using the new distant samples. In the local Universe, the on-going *Chandra* ESZ-XVP (PI Jones) is dedicated to full follow-up of the ESZ (PC11a), the initial *Planck* sample of 189 clusters with median redshift $\tilde{z} = 0.15$. A complementary *XMM-Newton* follow-up program (PI Forman) ensures full X-ray follow-up of the sample used in the *Planck* 2013 SZ cosmology paper (PC13c), which has $\tilde{z} = 0.18$. At higher redshift, 80 SPT clusters at $0.3 < z < 1.2$ were observed in a *Chandra* XVP (SPT-XVP; PI Benson, see Figure 1). An *XMM-Newton* large program (PSZ1 XMM-LP; PI Arnaud) was also initiated to follow-up the first objects at $z > 0.5$ in the first *Planck* catalogue PSZ1 (PC13b). These combined X-ray/SZ data are yielding new constraints on cluster scaling and structural properties and their evolution, in addition to information on the surveys themselves.

The *XMM-Newton* validation program (PC11b) provided a first view of the SZ-X-ray scaling properties and raised the first questions concerning the respective role of selection effects in X-ray and SZ surveys. The newly discovered SZ clusters appear to have a lower X-ray luminosity on average at given mass (PC13a), possibly reflecting a bias in X-ray surveys towards clusters with centrally peaked morphology. The ESZ-XVP observations show that there are less Cool Core Clusters in SZ selected sample than in X-ray selected sample (Jones *et al.*, priv. comm.). This confirms that selection effects depend on wavelength and must be fully mastered for understanding both the properties of the underlying population and for cosmological applications.

Nevertheless, there is a remarkable self-similarity of the pressure profiles over 4 orders of magnitude in radius as observed from combining *Planck* and *XMM-Newton* observations, providing new constraints on thermodynamic properties of the gas in cluster outskirts and on the physics of accretion (PC13a, see also Eckert *et al.* 2013). New results from the PSZ1-XMM-LP indicates that the pressure profiles evolve self-similarly, up to z = 0.7, with only a slightly less peaked core profile, as illustrated in the left panel of Fig. 2 (Arnaud *et al.* to be submitted), consistent with earlier work by McDonald *et al.* 2014 who found self-similarity out to $z \sim 1$ for the SPT-XVP sample. Consistently there is a very small dispersion in the $Y_{\rm X}$–$Y_{\rm SZ}$ relation at all redshift, supporting the view that both $Y_{\rm SZ}$ and $Y_{\rm X}$ are good mass proxies and putting upper limit on the gas clumpiness (PSZ1).

New *XMM-Newton* observations of a pilot sample of 4 Planck/SPT clusters at $z \sim 1$ are being used to explore the evolution of the integrated total mass profiles. First results show the capability of *XMM-Newton* to map the profiles up to R_{500} in a reasonable exposure time (< 150 ksec). They also indicate an evolution in the dispersion of the profiles but a larger data set is required for better quantification.

2. Probing the Evolution of the ICM with Joint X-ray-SZ Surveys

Michael McDonald presented results from the recently-completed South Pole Telescope (SPT) 2500 deg^2 survey, which found a total of 677 galaxy clusters spanning $0.2 < z < 1.7$, with a median redshift of $z = 0.55$ (Bleem *et al.* 2015). These SZ surveys provide

https://doi.org/10.1017/S1743921316004543 Published online by Cambridge University Press

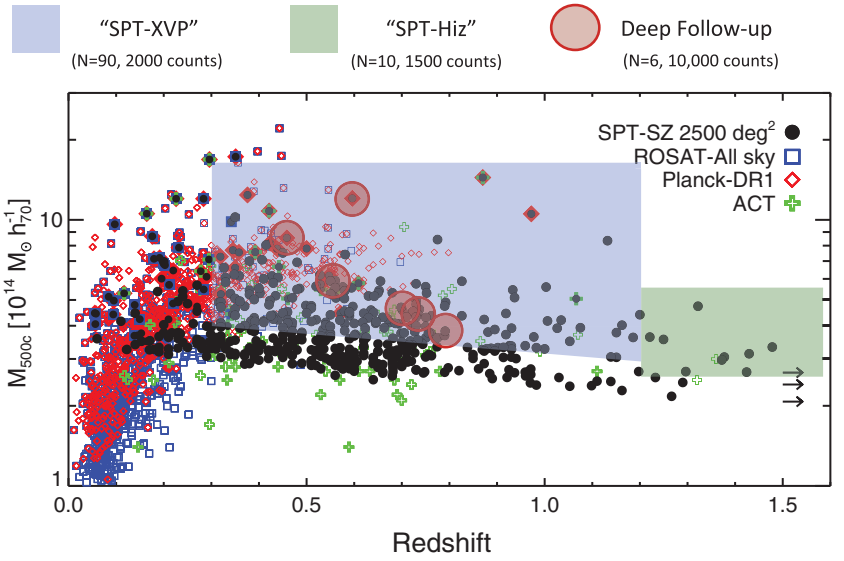

Figure 1. Mass vs redshift distribution for four different galaxy cluster surveys (legend in upper right). Black points show clusters selected by the South Pole Telescope, which uses the SZ effect to detect clusters in a redshift-independent way. Shaded blue, green, and red regions highlight the parameter space of three large *Chandra* follow-up programs, targeting "intermediate-redshift" ($0.2 < z < 1.2$), "high-redshift" ($1.2 < z < 1.7$), and relaxed clusters, respectively. Combined, these surveys probe the evolution of galaxy clusters in a (nearly) redshift independent way, both in selection and follow-up, allowing detailed studies of the intracluster medium over most of the lifetime of massive galaxy clusters.

a fertile ground for studying the evolution of galaxy clusters and galaxies in the cluster environment. However, very little astrophysics can be addressed with the SZ signal alone – we require follow-up with optical and X-ray telescopes in order to properly track the evolution of these systems.

The SPT collaboration has recently completed a comprehensive X-ray follow-up of ∼100 SPT-selected galaxy clusters spanning $0.25 < z < 1.7$ and with $M_{500c} \gtrsim 3 \times 10^{14}$ $M_\odot$. These observations, made with the *Chandra X-ray Observatory*, have exposure times chosen to provide ∼2000 X-ray counts per cluster, based on the L_X–M relation. This choice of exposure time, coupled with the SZ selection, yields a sample of galaxy clusters with X-ray observations which (I) are uniformly selected in mass, (II) have nearly uniform S/N, (III) have nearly uniform angular resolution (factor of ∼2 difference from $z = 0.25$ to $z = 1.5$), and (IV) span the bulk of the lifetime of a massive galaxy cluster. This follow-up strategy has allowed for some of the most comprehensive and unbiased studies of galaxy cluster evolution to date. These observations have been split over three large programs, led by PIs B. Benson (Cycle 13 XVP, 80 clusters at $0.25 < z < 1.2$), M. McDonald (Cycle 16 LP, 10 clusters at $1.2 < z < 1.7$), and J. Hlavacek-Larrondo (Cycle 17 LP, deep follow-up of 6 clusters), as outlined in Figure 1.

The primary results from the *Chandra*-SPT survey thus far concern the evolution of the ICM over the past ∼9 Gyr. McDonald *et al.* (2013) showed that the hot ICM in distant clusters is considerably less centrally concentrated than in nearby systems. That is, the classical picture of "cool-core" clusters exhibiting cuspy X-ray surface brightness profiles is a $z \sim 0$ phenomenon. On the other hand, the core entropy and cooling time, which depend on the gas density and temperature, appear to be redshift independent for $z \lesssim 1$. This implies that there has been a long-standing balance between cooling

https://doi.org/10.1017/S1743921316004543 Published online by Cambridge University Press

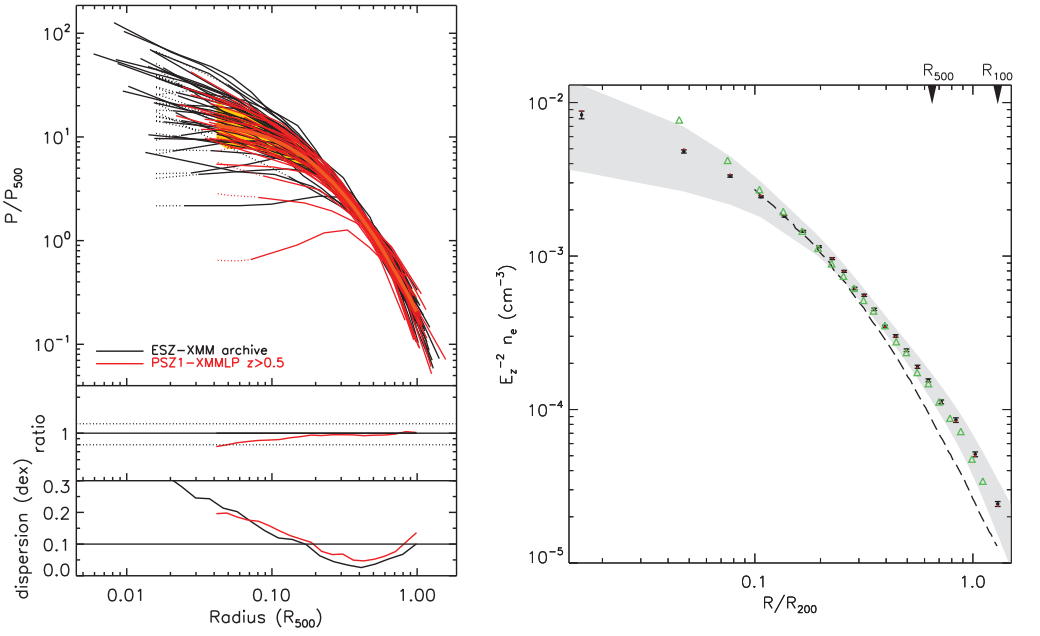

Figure 2. *Left panel:* Illustrative results of *XMM-Newton* data on *Planck* distant clusters at $0.5 < z < 0.7$ (PSZ1-XMM-LP). The scaled pressure profiles (red) are compared to local profiles (black) from archival data on *Planck* ESZ clusters (PC13a). There is no significant evolution in the dispersion about the mean (bottom panel) and only a slight evolution of the mean profile in the core. This results need to be confirmed via a comparison with a purely SZ selected local sample, such as that of the *Chandra* ESZ-XVP. *Right panel:* Average gas density profile for the whole sample. The points with errorbars represent the median values, while the red points represent the weighted average profile. Note that the errorbars refer to the errors on the median emission measure profiles, while the gray shaded region refers to the intrinsic scatter (68.3% confidence level), which amounts to $\sim 20\%$ ($\sim 30\%$) at R_{500}. The long dashed line represents the predictions from the hydrodynamic numerical simulations of Roncarelli *et al.* (2006), while the green triangles represent the universal gas density profile from Eckert *et al.* (2012) based on *ROSAT* data.

and feedback, with cluster cores "frozen" in a semi-cooled state for the past ∼9 Gyr. McDonald *et al.* (2014) performed a stacking analysis on the full sample of ∼90 clusters spanning $0.25 < z < 1.2$ and found that the average entropy *profile* interior to $r \sim 0.5R_{500c}$ is roughly constant for cool core cluster, implying a more large-scale balance between cooling and feedback. This work also provided the first measurement of the "Universal" pressure profile at $z \gtrsim 0.5$, showing that the profile is only uniform at radii where gravitational processes dominate over other astrophysics ($r \gtrsim 0.15R_{500c}$). Finally, recent work by Hlavacek-Larrondo *et al.* (2015) has shown evidence for strong radio-mode feedback in the cores of galaxy clusters out to $z \sim 1$, again suggesting a long-standing balance between cooling and feedback in cool core clusters. A follow-up program on these systems which show strong evidence for radio-mode feedback will allow a more precise quantification of mechanical power of the AGN, which can change by a factor of 2–3 with deeper observations (e.g., McDonald *et al.* 2015).

The follow-up of SPT-selected clusters with the *Chandra* X-ray Observatory combines the strengths of two great observatories. With uniform S/N X-ray observations of a mass-limited sample of clusters, the team is in a unique position to probe the evolution of galaxy clusters beyond the reach of previous surveys, free from many of the systematic biases that plagued earlier evolutionary studies. In the next year, McDonald *et al.* will

https://doi.org/10.1017/S1743921316004543 Published online by Cambridge University Press

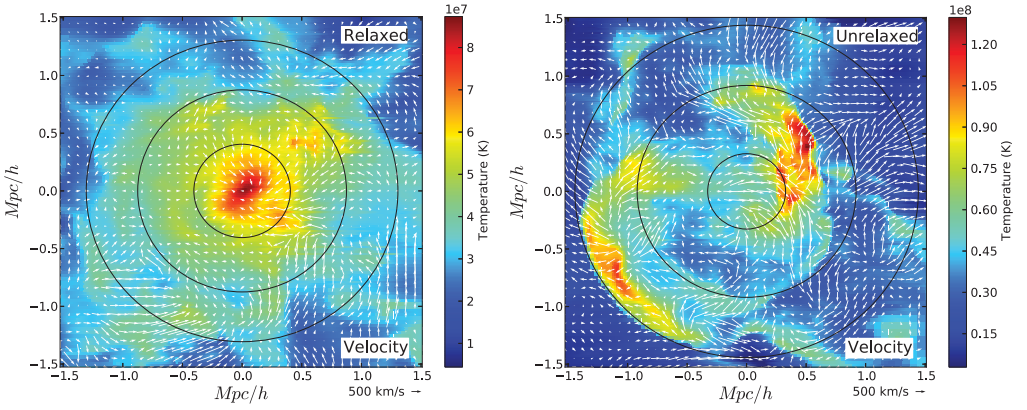

Figure 3. Projected mass-weighted temperature map of a relaxed (left) cluster and an unrelaxed (right) cluster with the velocity vector fields overlaid from the *Omega500* cosmological cluster simulation. The black circles denote R_{2500}, R_{500} and R_{200} of the clusters from inside to outside. Both the maps and vector fields are mass weighted along a 200 kpc/h deep slice centered on their respective cluster centers.

complete the follow-up of clusters at $1.2 < z < 1.7$, providing the first uniformly-selected sample of galaxy clusters spanning $0.25 < z < 1.7$. These surveys are rapidly approaching the formation epoch of these massive systems $z \sim 2.5$, allowing us a glimpse into the state of the ICM shortly after its assembly.

3. Physics of Galaxy Cluster Outskirts

In recent years, the exploration of galaxy cluster outskirts has emerged as one of the new frontiers for studying cluster astrophysics and cosmology. It is a new territory for understanding the physics of ICM and intergalactic medium (IGM), and it is particularly important for interpretation of recent X-ray and SZ observations and cluster mass estimates based on these observations. However, initial results from *Suzaku* X-ray and *Planck* microwave space missions were very puzzling. For example, the entropy profiles from *Suzaku* data appear to be significantly flatter than theoretical predictions from hydrodynamical simulations (e.g., Reiprich *et al.* 2013 for a review). The observed enclosed gas mass fraction in the Perseus cluster also exceeds the cosmic baryon fraction (Simionescu *et al.* 2011), which is at odd with the theoretical expectation.

Daisuke Nagai argued that the physics of cluster outskirts may be richer and more complex than previously anticipated. To investigate the origin of these tensions between theory and observations, he presented results from the high-resolution *Omega500* cosmological simulation of galaxy cluster formation, which consists of the mass-limited sample of 65 galaxy clusters with $M_{500c} \geqslant 2 \times 10^{14} M_{\odot}$ at $z = 0$ (Nelson *et al.* 2014) (see Fig. 3). Their simulation suggests that the outskirt of galaxy clusters at $R \gtrsim R_{500}$ is a "cosmic melting pot", where the cosmic materials are actively accreting and generating clumpy and turbulent medium which are filled with non-equilibrium electrons due to continuous accretion and mergers. If not accounted for, these poorly understood physics of galaxy cluster outskirts can lead to biases in the interpretation of X-ray and SZ measurements of galaxy clusters as well as cosmological constraints derived from these observations.

Specifically, Nagai showed that radially increasing gas clumping factor predicted by their simulation can lead to the overestimate of the gas density profile derived from X-ray data and cause the flattening of the observed entropy profiles at large radii (Nagai

https://doi.org/10.1017/S1743921316004543 Published online by Cambridge University Press

& Lau 2011, Zhuravleva *et al.* 2013). Non-thermal pressure provided by merger-induced gas motions also has significant impact on the thermodynamic properties of the ICM and introduces biases in the hydrostatic cluster mass estimates (Nelson *et al.* 2012, Lau *et al.* 2013, Nelson *et al.* 2014b) as well as scatter in the cluster scaling relations (Yu *et al.* 2015). In the outskirts of galaxy clusters, electron temperature can also become significantly lower than the mean gas temperature, because Coulomb collisions are insufficient to keep electrons and ions in thermal equilibrium. This deviation is larger in more massive and less relaxed systems, ranging from 5% in relaxed clusters to 30% for clusters undergoing major mergers (Rudd *et al.* 2009, Avestruz *et al.* 2015). The presence of non-equilibrium electrons leads to significant suppression of the SZ effect signal and an underestimate of the hydrostatic mass. Merger-driven, internal shocks may also generate significant populations of non-equilibrium electrons in the cluster core, leading to a 5% bias on the integrated SZ mass proxy during cluster mergers.

On the observational side, the recent ultra-deep *Chandra* XVP observation has revealed gas clumps and filaments in the outskirt of a nearby relaxed cluster, A133 (Vikhlinin *et al.* in prep), supporting the picture that the cluster outskirt is a "cosmic-melting pot". The upcoming ASTRO-H mission, which is scheduled to launch in 2016, will soon make a first direct measurement of the internal gas flows in nearby massive galaxy clusters, by measuring shifting and broadening of Fe lines, which should provide important test of merger-induced gas motions in galaxy clusters that are predicted to be significant in the concordance ΛCDM hierarchical structure formation model (Nagai *et al.* 2013, Ota *et al.* 2015). Recent developments in simulations and observations promise to improve our understanding of cluster astrophysics in the coming years, which in turn should enable the use of galaxy clusters as a cosmological probe.

4. Probing the Galaxy Cluster Outskirts with *Chandra*

Andrea Morandi presented the analysis of a sample of 320 clusters ($z = 0.056 - 1.24$) from the *Chandra* archive, focusing on the properties of the X-ray emitting gas in the outskirts of galaxy clusters (Morandi *et al.* 2015). In this work, the authors (I) analyzed the large archival dataset of *Chandra* clusters to trace the gas density and gas fraction of the intracluster gas out to R_{100}, (II) investigated the evolution of the physical properties as a function of dynamical state, redshift, cluster temperatures, as well as their azimuthal variation, and (III) compared their average density and gas fraction profiles to the results of numerical simulations of galaxy cluster formation. Specifically, the authors measured the median of the distribution of the (renormalized) emission measure profiles $EM(R/R_{200})$ to detect signal in the outer volumes and measured the typical gas density, gas slope and gas fraction.

Based on these analyses, Morandi *et al.* (2015) reported a steepening of the density profiles beyond R_{500}, with slope $\beta \sim 0.68$ at $r = R_{500}$ and $\beta \sim 1$ at $r \gtrsim R_{200}$. The results is consistent with the previous results obtained using *ROSAT* and *Chandra* data, but it is in tension with some recent results obtained by *Suzaku* telescope. Note further that the observed profiles are inconsistent with the results of numerical simulations that include gas cooling and star formation, which convert a large amount of gas into stars and result in a low gas density and gas mass fraction than the observed profiles even well outside cluster cores. Moreover, analyses of different subsamples did not exhibit the dependence of the gas density profiles with dynamical state, temperature, or redshift, suggesting that the self-similarity holds for the ICM in the virialization region in galaxy clusters. Furthermore, the team measured the hot gas mass fraction in galaxy clusters observed with *Chandra* out to R_{100}. After converting the hot gas fraction to the total baryon

https://doi.org/10.1017/S1743921316004543 Published online by Cambridge University Press

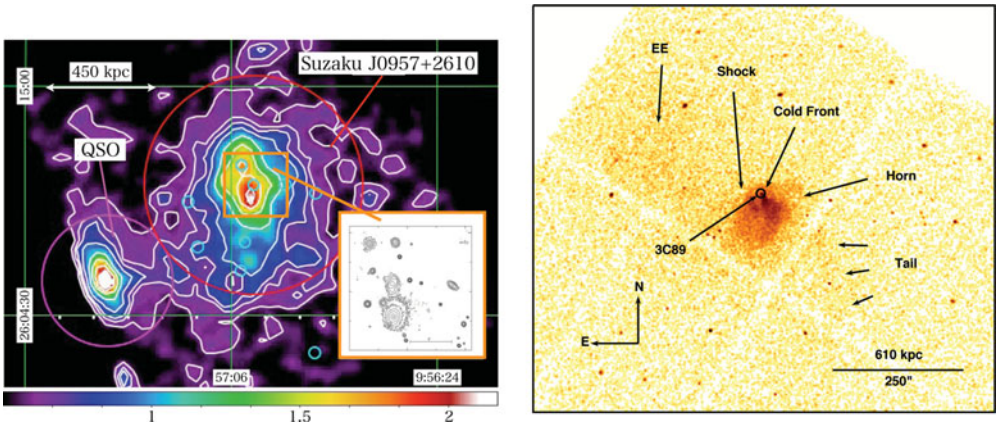

Figure 4. *Left panel: Suzaku* X-ray image in the 0.5–2.0 keV band (Mitsuishi *et al.* 2014). SDSS spectroscopic identified galaxies (cyan circle) and X-ray contours (white solid lines) are shown. Red and magenta circles correspond to regions that we extracted for spectral analysis. A close-up view of its central part in optical is also indicated as an orange rectangle (Tovmassian *et al.* 2005). *Right panel:* the count image of 66 ksec *Chandra* X-ray observation of the galaxy cluster RXJ0334.2-0111 (3C89) in the 0.7–7 keV band. Substructures discussed in this text are labelled by arrows.

budget in clusters, the authors found that the cluster baryon fraction which slightly exceeds the cosmic baryon fraction. However, a careful analysis of the systematics due to non-thermal pressure and clumpiness suggest that we might non-negligibly overestimate the total baryon budget, leading to an actual deficit of baryons in clusters with respect to the cosmic value. By tracking the direction of the cosmic filaments approximately with the ICM eccentricity, Morandi *et al.* report that galaxy clusters deviate from spherical symmetry, with only small differences between relaxed and disturbed systems.

5. Searching for Merging Groups of Galaxies with *Suzaku*

In the hierarchical structure formation model, merging process plays an important role in dynamical and chemical evolution of groups and clusters of galaxies over cosmic time. Despite the extensive studies for massive merging clusters (e.g., Govoni *et al.* 2004), observational samples of galaxy groups are limited due to its low surface brightness.

To address this issue, Ikuyuki Mitsuishi presented results from the ongoing observational program to search for merging galaxy groups (Kawahara *et al.* 2011, Mitsuishi *et al.* 2014). Using *Suzaku* X-ray observatory e.g., which possesses both high sensitivity especially in the soft energy band below 1 keV and stable background, the team conducted a search of merging groups in eight fields which are located around junctions of galaxy filaments and three optically-selected groups where an interaction between central and satellite galaxies. The team reported the discovery of five on-going major merging groups with temperature of $\sim$1-2 keV, abundance of $<$0.5 solar, and a luminosity of 10^{42-43} erg s^{-1}. Detailed spatial and spectral analyses further suggest that these galaxy groups possess complex morphology with multiple peaks in X-ray where no corresponding optically-bright early-type galaxies reside when the system is located around junctions of galaxy filaments. Furthermore, one of the observed X-ray halo shows an elongated feature and the direction is consistent with that of the observed systems in optical due to galaxy-galaxy interaction between the central and the second brightest galaxies (see

https://doi.org/10.1017/S1743921316004543 Published online by Cambridge University Press

the left panel of Figure 4). In fact, three group-size X-ray halos in six fields appear to be associated with major merger events.

Seven more *Suzaku* observations for five fields were performed to make our statements described above stronger. The first two fields are regions located around junctions of galaxy filaments and the others are SDSS optically-selected groups (McIntosh *et al.* 2008) with a mass of $10^{13.6-14.3}$ $M_\odot$ where a galaxy-galaxy merger between central and satellite galaxies occurs. Based on X-ray imaging and spectral analysis in conjunction with multi-wavelength observational results, the team concluded that we discovered two on-going major merging group-scale X-ray halos, one non-merging group, and one serendipitously-detected group as apparently diffuse X-ray sources (Mitsuishi *et al.* in prep.). As a next step, the authors plan to use the samples for understanding of a hierarchical structure formation in a transition phase from groups to clusters of galaxies.

6. Shocking Features in 3C89

Sarthak Dasadia presented a 66 ksec *Chandra* X-ray observation of a merging galaxy cluster RXJ0334.2-0111 (3C89), shown in the right panel of Figure 4. The *Chandra* observations show two prominent discontinuities in the surface brightness caused by the motion of the infalling subcluster. The authors find a region of high temperature surrounding the ram pressure stripped, bright, cool core marked by a sharp edge. This outer edge is confirmed to be a bow shock where the gas temperature increases by a factor of ~ 1.5 (from 4.1 keV to 6.2 keV upstream), and is consistent with the Mach number $M = 1.6^{+0.5}_{-0.3}$. The inner surface brightness edge that marks the border between infalling subcluster cool core and ICM of the main cluster is a cold front.

The temperature across the cold front increases from $1.3^{+0.3}_{-0.8}$ keV to $6.2^{+0.6}_{-0.6}$ keV. From the ratio of gas pressure between inside and outside the cold front they estimate that the cloud moves through the hot ambient medium at the velocity $\sim 1.5 \times 10^3$ km sec^{-1} which is close to the measured shock velocity of $1.6^{+0.6}_{-0.3} \times 10^3$ km sec^{-1}. Using the projected distance between two merger components and shock velocity, the authors estimate the time since the closest approach to be ~ 50 Myr. Dasadia *et al.* find an overpressurized region ~ 250 kpc east of the cold front that is named "the eastern extension (EE)". The EE may be a part of the third subcluster in the ongoing merger. They also find a tail shaped feature that originates near the bow shock and may extend up to a distance of ~ 1 Mpc. This feature is also likely overpressurized. The exceptionally luminous FR-I galaxy, 3C89, appears to be the cD galaxy of the infalling subcluster. Dasadia *et al.* estimated 3C89's jet power from jet bending and the possible interaction between the X-ray gas (Horn) and the radio lobes. Both methods gave similar results. RXJ0334.2-0111 adds a unique bow shock system associated with a wide angle tail (WAT) radio galaxy and several intriguing substructures.

References

Avestruz, C., Nagai, D., Lau, E., & Nelson, K., 2015, 808, 176
Bleem, L. E., Stalder, B., de Haan, T., *et al.* 2015, *ApJS*, 216, 27
Clerc *et al.*, 2014, *A&A*, *MNRAS*, 444, 2723
Eckert, D., Vazza, F., Ettori, S., *et al.* 2012, *A&A*, 541, 57
Eckert *et al.*, 2013, *A&A*, 551, A22 and A23
Govoni, F., Markevitch, M., Vikhlinin, A., *et al.* 2004, *ApJ*, 605, 695
Hasselfield *et al.*, 2013, JCAP, 7, 8
Hlavacek-Larrondo, J., McDonald, M., Benson, B. A., *et al.* 2015, *ApJ*, 805, 35

https://doi.org/10.1017/S1743921316004543 Published online by Cambridge University Press

Kawahara, H., Yoshitake, H., Nishimichi, T., Sousbie, T., *et al.* 2011, *ApJL*, 727, 38
K, Lau, E. T., Nagai, D., Avestruz, C. *et al.* 2015, *ApJ*, 806, 68
K, Lau, E. T., Nagai, D., & Nelson, K., 2013, *ApJ*, 777, 151
K, Lau, E. T., Kravtsov, A., Nagai, D., *et al.* 2009, *ApJ*, 705, 1129
Marriage *et al.*, 2011, *ApJ*, 737, 61
Mehrtens *et al.* 2012, *MNRAS*, 423, 1024
McIntosh, D. H., Guo, Y., Hertzberg, J., *et al.* 2008, *MNRAS*, 388, 1537
McDonald, M., Benson, B. A., Vikhlinin, A., *et al.* 2013, *ApJ*, 774, 23
McDonald, M., Benson, B. A., Vikhlinin, A., *et al.* 2014, *ApJ*, 794, 67
McDonald, M., McNamara, B. R., van Weeren, R. J., *et al.* 2015, *ApJ*, 811, 111
Mitsuishi, I., Kawahara, H., Sekiya, N., *et al.* 2014, *ApJ*, 783, 137
Mitsuda, K., Bautz, M., Inoue, H., *et al.* 2007, *PASJ*, 59, 1
Morandi, A., Sun, M., Forman, W., & Jones, C., 2015, *MNRAS*, 450, 2261
Nagai, D., Lau, E., Avestruz, C., *et al.* 2013, *ApJ*, 777, 137
Nelson, K, Rudd, D., Shaw, L., & Nagai, D., 2012, *ApJ*, 751, 121
Nelson, K, Lau, E. T., Nagai, D., *et al.* 2014a, *ApJ*, 782, 107
Nelson, K, Lau, E. T. & Nagai, D., 2014b, *ApJ*, 792, 25
Ota, N, Nagai, D., Lau, E. T., (arXiv:1507.02730)
Planck Collaboration, Planck Early result VIII, 2011, *A&A*, 536, A8
Planck Collaboration, Planck Early result IX, 2011, *A&A*, 536, A9
Planck Collaboration, Planck Early result XI, 2011, *A&A*, 536, A11;
Planck Collaboration, Planck Intermediate Result V, 2013, *A&A*, 550, A131
Planck Collaboration, Planck 2013 results XXIX 2013, *A&A*, 571, A29 and 2015, 581, A14
Planck Collaboration, Planck 2013 results XX 2013, *A&A*, 571, A20
Planck Collaboration, Planck 2015 results XXVII 2015, *A&A*, in press, [arXiv1502.01598]
Reiprich, T. H., Basu, K., Ettori, S. *et al.* 2013, *SSRv*, 177, 195
Rudd, D. & Nagai, D., 2009, *ApJ*, 701. 16
Roncarelli, M., Ettori, S., Dolag, K., *et al.* 2006, *MNRAS*, 373, 1339
Simionescu, A., Allen, S. W., Mantz, A., *et al.* 2011, *Science*, 331, 1576
Tovmassian, H. M., Tiersch, H., Tovmassian, G. H., *et al.* 2005, *RMxAA*, 41, 3
Yu, L., Nelson, K., & Nagai, D. 2015, *ApJ*, 807, 12
Zhuravleva, I., Churazov, E., Kravtsov, A., *et al.* 2013, *MNRAS*, 428, 3274